Hydrothermal Minerals Record CO_2 Partial Pressures in the Reykjanes Geothermal System, Iceland

Adam J. E. Freedman[1*], Dennis K. Bird[1], Stefán Arnórsson[2], Thráinn Fridriksson[3], Wilfred A. Elders[4] and Gudmundur Ó. Fridleifsson[5]

[1]Department of Geological and Environmental Sciences, Stanford University, Stanford, CA

[2]Science Institute, University of Iceland, Dunhagi 3, 107 Reykjavik, Iceland

[3]ISOR, Iceland GeoSurvey, Grensasvegur 9, 108 Reykjavik, Iceland

[4]Department of Earth Sciences, University of California, Riverside, CA

[5]HS-Orka, Ltd. Brekkustigur 36, 260 Reykjanesbaer, Iceland

*freedman.adam@gmail.com

ABSTRACT

The Reykjanes Peninsula in southwest Iceland is the landward extension of the Mid-Atlantic Ridge spreading center. At present seawater penetrates the coastal Reykjanes geothermal system at depth, mixes with magmatic volatiles and reacts with the basaltic host rock to form secondary geothermal minerals in progressively higher-grade mineral alteration zones with depth where highest recorded temperatures are ~320°C. Within the epidote-chlorite and portions of the epidote-actinolite zones of alteration, epidote-prehnite-calcite-quartz-fluid constitutes a quadra-variant assemblage that, under conditions of specified temperature, pressure, and activity of H_2O allows prediction of geothermal fluid P_{CO2} as a function of the composition of the solid solution minerals epidote or prehnite. This assemblage is most common at temperatures >250°C and <~310°C, and potentially provides a mineralogic chronometer constraining fluid CO_2 concentrations based on compositional zoning in hydrothermal epidote. Analysis of epidote crystals separated from drillhole-cuttings from three geothermal wells (RN-9, RN-10, RN-17) display complex chemical zoning, generally with Fe(III)-rich cores and Al-rich rims. The Fe(III)-mol fraction of epidote at depths between 0.5 to 1 km ranges from 0.21 to 0.38, between 1 to 2 km depth the range is 0.17 to 0.48 and between 2-3 km it is 0.17 to 0.30. The Fe(III)-mol fraction of prehnite ranges from 0.11 to 0.59 in the upper portions of drillhole RN-17. The highest Fe(III) content in epidote that was observed to co-exist with prehnite is an Fe(III)-mol fraction of 0.36, which serves as the upper Fe(III) limit for epidotes used in this study. Because most observed prehnite crystals in the drillhole-cuttings are too small for electron micropropbe analyses (<20μm), we employed a sigmoidal regression of available compositional data from active geothermal systems to calculate the Fe(III)-Al composition of prehnite using measured compositions of epidote in the Reykjanes system. Calculated values of P_{CO2} for the geothermal fluids using epidote compositions from crystals obtained from drillcutting at depths >600m between the reference temperatures of 275°C and 310°C range from ~1 to ~6.5 bars, when only epidote, prehnite and quartz are observed. When all members of the assemblage are present, including calcite, the calculated range in P_{CO2} is from ~0.5 to 6 bars. If calcite is absent from the assemblage, the computation of P_{CO2} using equilibria for reaction 1 provides the maximum value of P_{CO2} at which calcite will not be present. Actual P_{CO2} values of geothermal fluids from the Reykjanes system were derived from analytical data on liquid and vapor samples collected at the surface using both the WATCH and SOLVEQ speciation programs. The geothermal fluids at reference temperature between 275°C and 310°C have P_{CO2} concentrations ranging from 1.3 bars to 4.0 bars.

The calculated P_{CO2} values based on epidote compositions are in close agreement with present-day measured CO_2 in the Reykjanes geothermal system fluids. 74% of the calculated P_{CO2} values based on epidote compositions where the complete epidote-prehnite-calcite-quartz assemblage is observed fall within the range of measured present-day fluids, while 62% of the calculated P_{CO2} values fall within the range when calcite is not present in the assemblage. Therefore, our method for calculating fluid P_{CO2} is proven quite reliable when all four index minerals are present. Additionally, if only epidote, prehnite and quartz are observed, our method still serves as a moderately accurate predictive proxy for fluid P_{CO2} composition in the Reykjanes geothermal system. Ultimately, the correlation between measured and predicted fluid compositions, provides insight into future abilities to characterize spatial and temporal concentrations of CO_2 in active and fossil hydrothermal and low-grade metamorphic environments in mafic lithologies based on compositional variations and paragenesis of hydrothermal minerals. In addition, this study will aid in understanding the nature of reactions that involve natural sequestration of CO_2 derived from magmatic degassing, and injection of industrial CO_2-rich fluids within hydrothermal environments in basaltic rocks.

1. INTRODUCTION

Mid-ocean ridge spreading centers represent a significant natural source of CO_2 from the Earth's mantle due to degassing from upwelling magma. The global mid-ocean ridge CO_2 flux is estimated to be between 1 and $3\bullet10^{12}$ mols/year (Marty and Tolstikhin, 1998; Sleep and Zahnle, 2001). Iceland is one of the few places on Earth where this magmatic-hydrothermal environment occurs above sea level (Fig. 1). Upwelling magma related to the spreading center and the Iceland Mantle Plume at the exposed ridge is responsible for the formation of Iceland at the center of the North Atlantic Igneous Province (Fig. 1a; Arnórsson, 1995); White and Morton,1995; Conrad et al., 2004). Presently the rift zones in Iceland are characterized by volcanic, seismic and geothermal activity (Pálmason et al., 1985). There are more than twenty high-temperature geothermal systems (>200°C at <1 km depth), including the Reykjanes system in

southwest Iceland (Arnórsson, 1995). Fluid and mineral samples recovered from deep drillholes at the Reykjanes geothermal system permit investigation of mineralogic phase relations that are potential indicators of the concentration of CO_2 released from the magmatic heat source to fluids in the geothermal system.
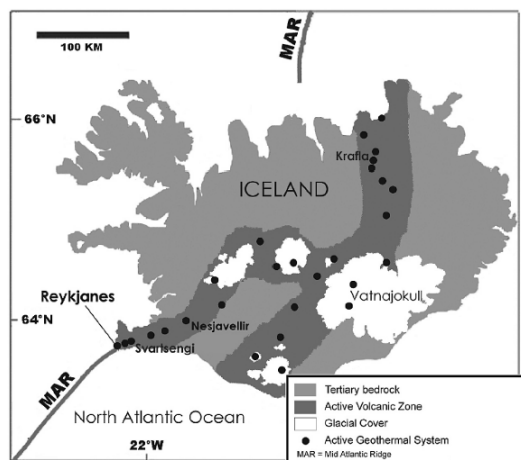

Figure 1a: The distribution of active high-temperature geothermal systems in Iceland. (Adapted from Larsen et al., 1998; Arnórsson, 1995)

This geothermal system occurs mainly within basaltic rocks including hyaloclastites, breccias, tuffaceous sediments, lava flows, and pillow lavas (Tómasson and Kristmannsdóttir, 1972). The present day geothermal fluid input is comprised of seawater that has been modified by the addition of magmatic gases and reaction with the host basalts, as well as boiling in the upflow zone (above ~1200 m depth at present); the water-rock interaction has resulted in the formation of a series of mineral alteration zones that increase in grade with depth (see review in Arnórsson, 1995; Bird and Spieler, 2004). These alteration zones are defined by the predominance of a single or several specific secondary minerals as illustrated in Figure 2 (Franzson et al., 2002; Fridleifsson et al., 2005).
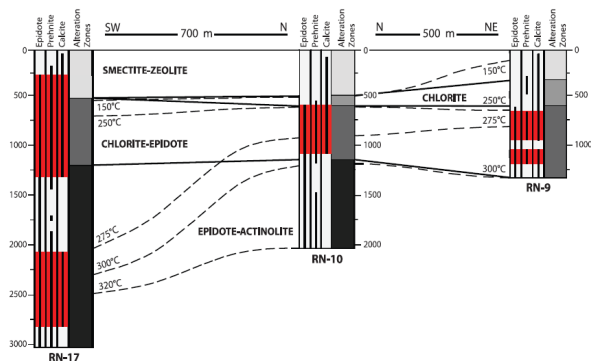

Figure 2: Cross-section through RN-9, RN-10, and RN-17, including mineral alteration zones, distribution of epidote, prehnite and calcite, and isotherms. Distribution of epidote, prehnite and calcite is denoted by the vertical black lines for wells RN-9, RN-10, and RN-17. The geothermal alteration zones are represented by different shades of gray for each drillhole and are connected by solid lines (Adapted from Hjartarson and Júlíusson, 2007)

Hydrothermal minerals found within the chlorite-epidote and epidote-actinolite alteration zones (see Fig. 2) include adularia, albite, anhydrite, calcite, garnet, prehnite, pyrite, and quartz in addition to the minerals characterizing the alteration zones.
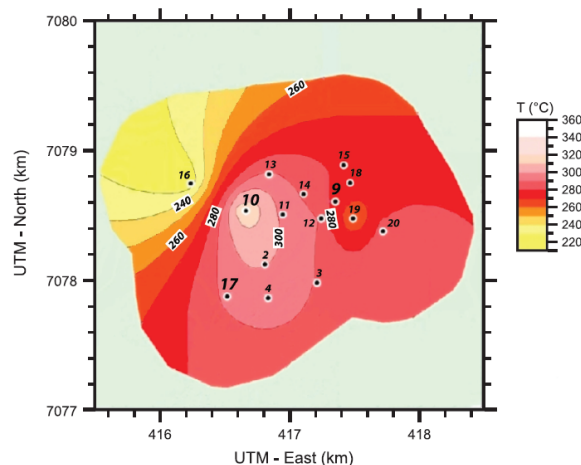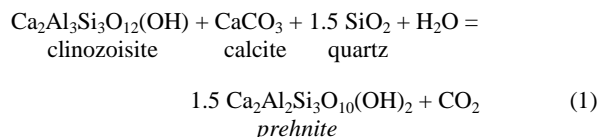

Figure 1b: Map of the Reykjanes drill field showing location of drillholes (by number) and isotherms (°C) at 2200 m depth based on available temperature logs. RN-10 is at the center of the thermal anomaly, RN-17 is to the south and RN-9 to the east (Adapted from Hjartarson, 2006)

Calcite is abundant in all wells in the uppermost ~1 km of the system, and occurs sporadically at greater depths. Potentially, several mineral assemblages that include calcite could buffer CO_2 concentrations in the geothermal system (Arnórsson et al., 2007).

Here we focus on a common mineral assemblage found in the Reykjanes geothermal system that consists of Fe(III)-Al epidote, Fe(III)-Al prehnite, calcite and quartz as a possible CO_2 buffer (cf. Arnórsson and Gunnlaugsson, 1985). For thermodynamic calculations we represent this assemblage by the stoichiometric reaction:

$$Ca_2Al_3Si_3O_{12}(OH) + CaCO_3 + 1.5\ SiO_2 + H_2O =$$
$$\text{clinozoisite} \qquad \text{calcite} \qquad \text{quartz}$$

$$1.5\ Ca_2Al_2Si_3O_{10}(OH)_2 + CO_2 \qquad (1)$$
$$\textit{prehnite}$$

where $Ca_2Al_3Si_3O_{12}(OH)$ represents the component corresponding in composition to clinozoisite in Fe(III)-Al epidote solid solutions, and $Ca_2Al_2Si_3O_{10}(OH)_2$ denotes the Al-end-member component in Fe(III)-Al prehnite solid solutions. At specific temperature, pressure, and activity of liquid water (our chosen standard state for the component H_2O), the equilibrium constant relationship for the reaction (1) in the system $NaCl-CaO-Al_2O_3-Fe_2O_3-SiO_2-H_2O-CO_2$ allows prediction of local equilibrium constraints between carbon dioxide (CO_2) concentrations (represented by either aqueous concentrations or the partial pressure of CO_2; we chose the gas standard state for CO_2 in this study, see below) in geothermal fluids and the Fe(III)-Al composition of either epidote or prehnite.

2. REYKJANES GEOTHERMAL SYSTEM

Temperature distribution at 2000 m depth within the Reykjanes geothermal system is shown in Figure 1b. Of the wells specifically considered for the present study, RN-10 is located within the center of the present-day thermal

anomaly, while RN-9 is located about 500 m to the east and RN-17 is located approximately 700 m to the south on the flank of the anomaly. Temperatures are in excess of 250°C below ~0.5 km depth in the hottest part of the field, below which the fluids closely follow the seawater boiling point curve for a few hundred meters. At greater depths the fluids remain *sub-boiling*, increasing in temperature only marginally with depth to the bottom of the drillholes (Hjartarson and Juliusson, 2007).

As we have chosen in this study to represent the chemical potential of CO_2 in the geothermal fluids with the descriptive variable of the partial pressure of CO_2 (P_{CO_2}), we note that reported values computed from combined analysis of vapor and liquid well discharges are 0.943 bars at 244°C (Stefánsson and Arnórsson, 2002), and between 1.56 to 2.59 bars at reference temperatures of 270 to 295°C (Lonker et al., 1993). Below we report data and computations indicating geothermal reservoir P_{CO_2} values in the range of ~1.3 to 4 bars over the reference temperature range of 275 to 310°C.

Reaction of geothermal fluids with the basaltic host rocks has formed a series of progressively higher grade alteration zones with depth, each characterized by distinct mineral assemblages and categorized by the presence of one or more index minerals including smectite, zeolites, chlorite, epidote and actinolite (Fridleifsson et al., 2005; Franzson et al., 2002, Franzson, 2000; Lonker et al., 1993). As illustrated in Figure 2 these alteration zones are consistently observed at approximately similar depths at RN-9, RN-10 and RN-17 (Fridleifsson et al., 2005; Franzson et al., 2002; Franzson, 2000; Lonker et al., 1993; Mungania, 1993). The depth ranges where epidote, prehnite, calcite and quartz have all been identified in drill cuttings from wells shown in Figure 1b are shown graphically by the red colored bars in the cross section of Figure 2.

3. MINERAL CHEMISTRY OF EPIDOTE AND PREHNITE

Epidote has a formula of $Ca_2Fe_xAl_{3-x}Si_3O_{12}(OH)$, where x represents the number of atoms of Fe(III) substituted for Al in the M1 and M3 crystallographic sites. Several studies have shown that the Fe(III) atoms are distributed almost exclusively in the largest and most distorted M3 site, and to a lesser extent in the M1 site. Rarely, and only at high temperature does Fe(III) enter the M2 site, which under the vast majority of conditions contains only Al (Dollase, 1973; Bird et al., 1988; Patrier et al. 1991; Giuli et al., 1999; Gottschalk, 2004).

Two common end-members components of epidote solid solutions are *clinozoisite* ($Ca_2Al_3Si_3O_{12}(OH)$) and *epidote* ($Ca_2Al_2FeSi_3O_{12}(OH)$); most natural epidotes are compositionally between these end-members. The composition of Fe-epidote ($Ca_2Fe_3Si_3O_{12}(OH)$), referred to as *pistacite*, does not occur in nature, but is a useful theoretical end-member for natural epidotes more Fe(III)-rich than ($Ca_2Al_2FeSi_3O_{12}(OH)$). The notation of X_{ps} is used here to denote the mole fraction of the *pistacite* component in natural epidotes, where X_{ps} is equal to $n_{Fe}/(n_{Fe} + n_{Al})$ and n_{Fe} and n_{Al} represent the number of atoms of Fe and Al per formula unit respectively.

Epidote commonly forms in active geothermal systems as the product of reactions between hydrothermal solutions and Ca-bearing phases in the host rocks, such as plagioclase or calcite (Arnason et al., 1993; Bird and Spieler, 2004). In the basalt hosted geothermal systems of Iceland, epidote typically occurs as yellowish green, xenoblastic crystals (<0.8 mm) and as radiating crystal aggregates (25–250 μm) often replacing plagioclase and filling vesicles and veins as a secondary alteration mineral (Tómasson and Kristmannsdóttir, 1972; Sveinbjörnsdóttir, 1992; Ragnarsdóttir et al., 1984; Lonker et al., 1993; Bird and Spieler, 2004).

Prehnite has the general stoichiometry of $Ca_2Al_{1-x}Fe_x(AlSi_3O_{10})(OH)_2$ where x denotes moles of Fe(III) substitution for octahedral Al. Other than Fe(III) substitution in the M1 site, which has been reported as high as 60 mole percent (Deer et al., 1962; Hashimoto, 1964; Surdam, 1969). Prehnite commonly occurs as a secondary mineral in basalt and related rocks (Klein, 2002). Prehnite has been observed in trace quantities in drill cuttings from all the drillholes in the Reykjanes geothermal system (Mungania, 1993; Lonker et al., 1993; Franzson, 2002, Fridleifsson et al., 2005). It typically occurs as light green, sheaf-like aggregates in open space fillings and veins that have been found to crosscut albite veins.

4. COMPOSITION OF EPIDOTE AND PREHNITE

4.1 Analytical Procedures

Electron microprobe analyses were used to determine the mineral chemistry of epidote and prehnite, particularly with regard to octahedral substitution of Al and Fe(III) (Fig. 3b). Analyses were conducted on an automated JEOL 733A electron microprobe at Stanford University operated at 15 kV accelerating potential and 15 nA beam current. Calibration was conducted using natural geologic standards. Beam diameter for analysis of epidotes and prehnites was 2-3 microns. Raw counts were collected for 20 s (approximately 60 s total beam contact at each point) and element distribution was converted to oxide percents and formula atoms based on 12.5 oxygens for epidote and the 11 oxygens for prehnite.

4.2 Epidote Composition

Analyzed compositions of epidote and the corresponding mole fraction of the Fe(III) endmember, X_{ps} ($X_{ps} = n_{Fe}/(n_{Al} + n_{Fe})$), from RN-9, RN-10 and RN-17 are shown graphically in Figure 6 as a function of depth. RN-9 epidotes display strong core-rim zoning with Fe(III)-rich cores and Al-rich rims at all depths, though to a greater extent with depth. The analyzed RN-9 epidotes from above 1 km depth exhibit an X_{ps} range of 0.21 to 0.34, while the X_{ps} values of samples from below 1 km depth extend from 0.19 to 0.44. The RN-10 epidotes from 1 to 2 km depth also have Al-rich rims and Fe(III)-rich cores and compositions range from X_{ps} of 0.18 to 0.48.

In RN-17, above 1 km depth, epidotes are all mostly Fe(III)-rich, ranging in a similar fashion to RN-9 samples from an X_{ps} of 0.24 to 0.38. From 1 to 2 km depth, however, the samples exhibit Fe(III)-rich core and Al-rich rim zoning and the compositions extend over a wider range from X_{ps} of 0.21 to 0.46. These values are very similar to the compositional range observed in both RN-9 and RN-10 at the same depths. The RN-17 samples from 2 to 3 km depth do not exhibit the dramatic Al-Fe(III) zoning. Unlike the shallow Fe-rich samples, epidotes formed at > 2 km depth do not exhibit such high Fe(III) concentration and range from X_{ps} of 0.17 to 0.36. The X_{ps} range from 2 to 3 km depth RN-17 displays a similar Fe(III) distribution to the *rims* of epidotes from 1 to 2 km depth in RN-10 and RN-17. On the other hand, the X_{ps} range of the < 1.0 km depth RN-17 epidotes display a similar Fe(III) content to that of epidote *cores* at depths of 1 to 2 km in both RN-10 and RN-17.
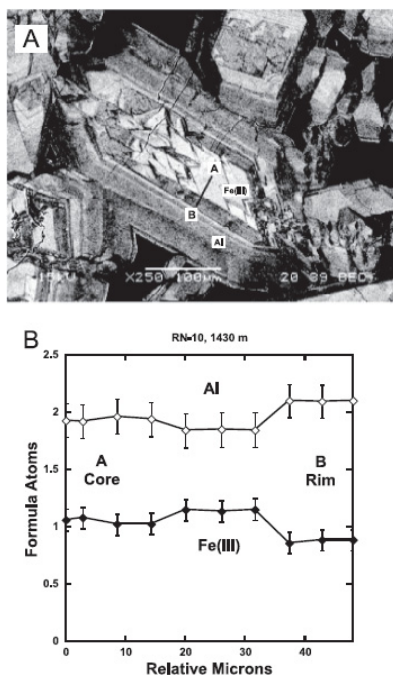
Figure 3: a) Back-scattered electron photomicrograph showing complex oscillatory zoned epidote The line traversing the image shows the traverse of the probe scan in which data was gathered approximately every 5.5 microns (see Fig. 4b). b) Quantitative analysis of microprobe scan reflecting relative amounts of Al (open diamonds) and Fe(III) (filled diamonds) as scan progressed across the crystal shown in Figure 4a

4.3 Prehnite Composition

Analyses of Al and Fe(III) content in prehnite samples from RN-17 are shown in Figure 5 (open squares with diagonal lines) as a function of depth. The prehnite compositions ($X_{Fe,Prehnite} = n_{Fe}$) in RN-17 at depths of 700 and 800 m range from $X_{Fe,Prehnite}$ of 0.13 to 0.59. A similar compositional range of $X_{Fe,Prehnite}$ of 0.15 to 0.55 is reported by Marks et al. (personal communication, 2006) at a depth of 550 m in RN-17, and Lonker et al. (1993) report a compositional range of $X_{Fe,Prehnite}$ between ~0.08 and 0.28 from drillholes RN-8 and RN-9 Measured prehnite compositions demonstrate an extreme range of Fe(III)-Al substitution similar to that of epidotes in the Reykjanes geothermal system.

5. THERMODYNAMIC CONSIDERATIONS

5.1 Phase Rule Constraints and Thermodynamic Conventions

Equilibrium for the assemblage epidote-prehnite-calcite-quartz-fluid, as represented by reaction (1), is used to evaluate the relationship between fluid CO_2 content and epidote composition. First we consider phase rule constraints:

$$f = c + 2 - p \qquad (2)$$

where f is the variance (independent variables), c is the minimum number of chemical components and p is the number of phases. Equilibrium denoted by reaction (1) for the Reykjanes geothermal system can be represented using 7 components (NaCl, CaO, Al_2O_3, Fe_2O_3, SiO_2, H_2O, and CO_2) to describe the compositions of the 5 phases (calcite, epidote, prehnite, quartz, and fluid) such that equation (2) becomes f = 7 + 2 − 5 = 4.
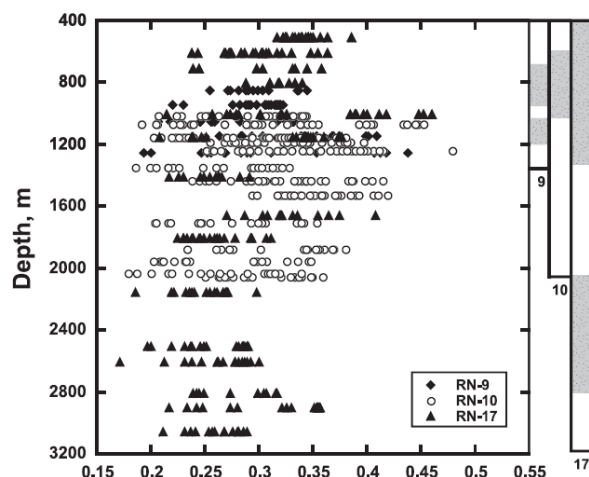

Figure 4: Compilation of epidote X_{ps} (n_{Fe} /($n_{Al} + n_{Fe}$)) as a function of depth from wells RN-9, RN-10 and RN-17. Gray bars to the right indicate the depths in wells RN-9, RN-10 and RN-17 where fragments of epidote, prehnite, quartz and calcite have been observed in drill cuttings
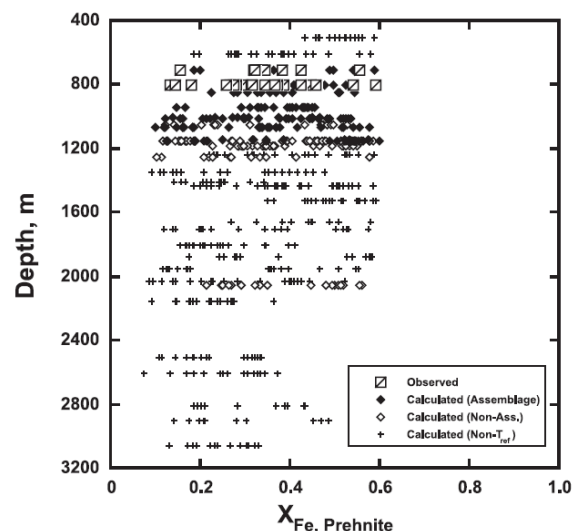

Figure 5: Calculated (diamonds) and measured (squares) $X_{Fe,Prehnite}$ values as a function of depth in wells RN-9, RN-10 and RN-17. The measured values are from RN-17, but the calculated values have been derived from epidote compositions in RN-9, RN-10 and RN-17 using equations 16 and 20. The solid diamonds (assemblage) are computed from measured compositions of epidotes at depths where prehnite, quartz and calcite are also found in the drill cuttings, and the open diamonds (non-assemblage) are from depths where prehnite and/or calcite are absent from the cuttings. Only samples found in cuttings at depths where reference temperatures range between 274 and 310°C are denoted as "assemblage" or "non-assemblage." All other values are labeled as "Non-T_{ref}."

The assemblage is quadra-variant; by fixing four intensive variables (e.g. temperature, pressure, the activity of H_2O in the fluid phase, and either epidote or prehnite composition), the equilibrium is uniquely defined. In the present study, observed temperature and pressure profiles in wells are constrained as a function of depth in the drillholes, activity

of H_2O is computed using aqueous species distribution algorithms and the composition of the geothermal fluid (see below), and epidote compositions are measured by microprobe analysis of crystals obtained from drillhole cuttings (the composition of prehnite is computed from equations and data given below) to calculate the fugacity of CO_2 in the geothermal fluids in equilibrium with this assemblage (see details below).

The following standard state conventions are adopted: unit activity of pure minerals and liquid H_2O at any temperature and pressure, and for CO_2 unit fugacity of the pure gas at 1 bar and any temperature (cf. Helgeson et al., 1978). The latter standard state chosen for CO_2 facilitates comparative analysis between values determined from drillhole discharge fluids and mineralogic constraints (reaction 1). We take the activities of $CaCO_3$ and SiO_2 components in calcite and quartz, respectively, to be equal to unity, and for the activity of H_2O in the geothermal fluid we use a value of 0.985 computed by the aqueous geochemical system modeling program, SOLVEQ and CHIM-XPT codes (formerly CHILLER, Reed, 1982), using the average composition of geothermal fluid from well RN-8, as reported by Arnórsson (1978; see below).

The equilibrium constant, K, for reaction (1) adopted in this study is computed using a temperature-dependent algorithm provided by Arnórsson et al. (2007: Log K = 57.781 - $22843/T^2$ - 4792.99/T + 0.00829 T + $0.6864 \times 10^{-6} T^2$ - 19.302 logT). The algorithm was derived using thermodynamic properties of minerals reported by Holland and Powell (1998), for H_2O from the SUPCRT computer program (Johnson et al., 1992), and for $CO_{2,g}$ from Robie and Hemingway (1995), at temperatures corresponding to liquid-vapor equilibrium for H_2O. Assuming, as a first order approximation, ideal gas behavior for CO_2, the equilibrium constant relationship for reaction (1) can be expressed as:

$$\log P_{CO2} \approx \log f_{CO2} =$$

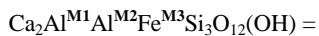$$\log K_{T,P} + \log a_{Czo} - 1.5 \log a_{Preh} + \log a_{H2O}, \quad (3)$$

where P_{CO2} is the partial pressure of CO_2 and f_{CO2} the fugacity of CO_2 in the geothermal fluid, $K_{T,P}$ is the equilibrium constant for reaction (1), a_{Czo} is the thermodynamic activity of the clinozoisite component in epidote, a_{Preh} is the thermodynamic activity of Al-prehnite in prehnite, and a_{H2O} is the activity of H_2O referenced to the liquid standard state described above. For $CO_{2,g}$ under low pressures of geothermal environments, we assume as a first order approximation that $f_{CO2} \approx P_{CO2}$.

5.2 Activity-Composition Relations

5.2.1 Epidote

If one designates completely 'ordered' epidote as containing Fe(III) in only the M3 site, then the octahedral 'disordering' of epidote that induces crystal lattice distortion with increasing temperature can be represented by:

$$Ca_2Al^{M1}Al^{M2}Fe^{M3}Si_3O_{12}(OH) =$$

$$Ca_2(Al_{1-x}Fe_x)^{M1}Al^{M2}(Al_xFe_{1-x})^{M3}Si_3O_{12}(OH), \quad (4)$$

such that x represents the mole fraction of Fe(III) in the M1 sites. Bird and Helgeson (1980) and Gottschalk (2004) represent the intracrystalline exchange reaction for Al and Fe(III) between the M1 and M3 sites within epidote by:

$$Fe(III)_{M3} + Al_{M1} = Fe(III)_{M1} + Al_{M3}, \quad (5)$$
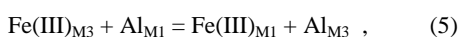
such that:

$$(X_{Fe,M1} \cdot X_{Al,M3}) / (X_{Fe,M3} \cdot X_{Al,M1}) = K', \quad (6)$$

where K' represents the 'intracrystalline equilibrium constant' for reaction (5) (see Bird and Helgeson (1980) for intracrystalline standard state conventions adopted). The values of K' are computed for epidote solid solutions at various temperatures by the relationship:

$$\log K' = -1523.4 \left(\frac{1}{T} - \frac{1}{T_r} \right) - 5.0, \quad (7)$$

where T is the temperature of the system and T_r is the reference temperature of 298.15 K (25°C).

Assuming ideal mixing of Al and Fe(III) on the M1 and M3 sites, the thermodynamic activity of the clinozoisite ($Ca_2Al_3Si_3O_{12}(OH)$) component of epidote solid solution can be computed by:

$$a_{Czo} = X_{Al,M1} \cdot X_{Al,M3}, \quad (8)$$

where $X_{Al,M1}$ is the mole fraction of Al in the M1 site and $X_{Al,M3}$ is the mole fraction of Al in the M3 site (Bird and Helgeson, 1980).

Based on total measured Fe(III) content of epidote (n_{Fe}), equation (5) is rearranged to determine the distribution of the Al and Fe(III). Since:

$$X_{Fe,M1} = n_{Fe} - X_{Fe,M3}, \quad (9)$$

$$X_{Fe,M3} = n_{Fe} - X_{Fe,M1}, \quad (10)$$

$$X_{Al,M3} = 1 - X_{Fe,M3}, \quad (11)$$

and

$$X_{Al,M1} = 1 - X_{Fe,M1}, \quad (12)$$

equation (6) can be expressed in terms of the intracrystalline equation constant, K' (equation 7), the measured total Fe(III), n_{Fe}, and the mole fraction of Fe(III) in the M3 site:

$$K'_{T,P} = \left(\frac{(n_{Fe} - X_{Fe,M3})(1 - X_{Fe,M3})}{X_{Fe,M3}(1 - (n_{Fe} - X_{Fe,M3}))} \right) \quad (13)$$

where n_{Fe} represents the total number of moles of Fe(III) per formula unit in the analyzed epidote. Equation (13) can then be reduced to the quadratic equation:

$$0 = (1-K') \cdot X_{Fe,M3}^2 - (1 + n_{Fe} - K'(1-n_{Fe})) \cdot X_{Fe,M3} + n_{Fe} \quad (14)$$

Calculated values of $X_{Fe,M3}$ using equation (14) and measured n_{Fe} allows determination of $X_{Fe,M1}$, $X_{Al,M3}$, and $X_{Al,M1}$ using equations (9), (10), (11) and (12) and thus the calculation of a_{czo} by equation (8).

5.2.2 Prehnite

The activity of the $Ca_2Al(AlSi_3O_{10})(OH)_2$ component in Fe(III)-Al prehnite solid solutions used in equation (3) is computed with an ideal site mixing approximation of:

$$a_{Preh} = X_{Al,Prehnite}, \quad (15)$$

where $X_{Al,Prehnite}$ is equal to the mole fraction of octahedral Al (Bird and Helgeson, 1980). In order to determine a

relationship between epidote and prehnite compositions a sigmoidal regression was employed to fit a data set consisting of the coexisting epidote and prehnite compositions from active geothermal systems reported Bird et al. (1984) and Milodowski et al. (1989), together with compositional constraints from mineral analyses of drill cuttings from the Reykjanes geothermal system reported by Lonker et al. (1993), Marks et al. (in review), and the present study (see Fig. 6 for details). The regression is subject to the compositional constraints that epidote with X_{ps} = 0 coexists with prehnite of $X_{Fe,Prehnite}$ = 0, and that the most Fe(III)-rich epidote (X_{ps} = 0.36), coexists with the most Fe(III)-rich prehnite ($X_{Fe,Prehnite}$ = 0.60) as measured from drill cuttings from well RN-17 at 700 and 800m depth (this study; see Fig. 9). The computed compositional relationship between X_{ps} and $X_{Fe,Prehnite}$ is:

$$X_{Fe,Prehnite} = 0.9903/(1 + \exp(-(X_{ps} - 0.3321)/0.0641)) \quad (16)$$

(Fig. 9). And since Fe(III) substitutes for Al in one octahedral site of prehnite, then:

$$X_{Al,Prehnite} = 1 - X_{Fe,Prehnite} =$$
$$1 - (0.9903/(1 + \exp(-(X_{ps} - 0.3321)/0.0641))). \quad (17)$$

Compositions of prehnite computed using equation (17) and the measured compositions of epidote (and Fig. 4) are shown in Figure 5 as a function of depth. Both the calculated and measured prehnite compositions represent similar values and ranges of Al and Fe, providing some degree of confidence in the use of calculated prehnite compositions in evaluating equilibrium for reaction (1). Thus, using equations (15) and (17) to calculate $X_{Al,Prehnite}$ values for every epidote analysis enables the calculation of a_{Preh} for each theoretically coexisting prehnite crystal.
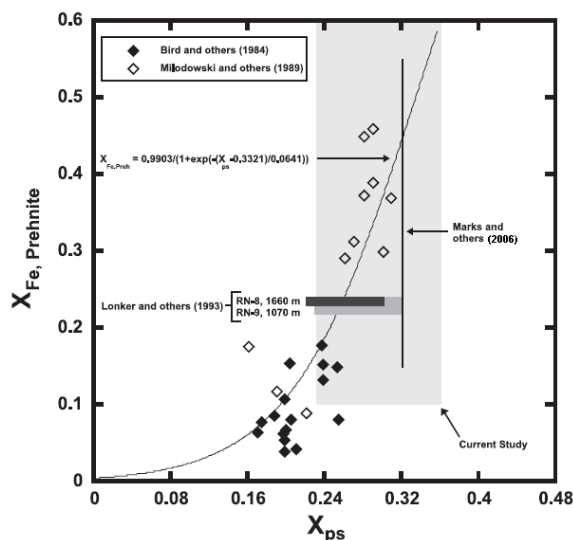

Figure 6: Compositional relations of Fe(III)-Al partitioning between epidote (X_{ps}) and prehnite ($X_{Fe,prehnite}$) in the Cerro Prieto geothermal system, Mexico (Bird et al., 1984), Miravales geothermal system, Costa Rica (Milodowski et al., 1989), and the Reykjanes geothermal system, Iceland (ranges of compositions reported by Lonker et al., 1993; Marks et al., in review; and present study). The gray curve denotes compositional relations consistent with Equation (17)

5.3. Equilibrium Constraints on P_{CO_2}

In equation (3) the activity of the Al-prehnite component (a_{Preh}) is computed using equations (15) and (17) as described above. The results are shown in Figure 7 at constant temperatures of 275°, 300° and 325°C for pressures equal to liquid-vapor equilibrium of H_2O. It is apparent from the diagram that equilibrium constraints imposed by reaction (1) requires P_{CO_2} increases with decreasing X_{ps} at constant temperature, and at constant X_{ps}, P_{CO_2} increases with increasing temperature, but to a lesser degree with increasing Fe(III) content in epidote. Inflections in the curvature of the isopleths in Figure 8 are an artifact of the sigmoidal regression of the data in Figure 6 and the temperature dependence of substitution order-disorder in epidote solid solutions.

6. CALCULATION OF AQUIFER FLUID COMPOSITION

Most modern geothermal fluid analyses for this study come from the Iceland GeoSurvey database, where the WATCH computer program (Arnórsson et al., 1983), version WDENS23 (Bjarnason, 1994) was used to compute the composition and aqueous speciation of the deep fluid. Calculated P_{CO_2} from geothermal fluid analyses are between 1.3 and 4.0 bars at reference temperatures between 275 and 310°C (see Figure 10a). Alternate values of deep fluid P_{CO_2} from the Reykjanes geothermal systems were computed for five chemical analyses from the Iceland GeoSurvey data base from wells RN-10, RN-12, RN-19, RN-21, and RN-23 using the SOLVEQ and CHIM-XPT codes (formerly CHILLER; Reed, 1982; Fig. 11a).
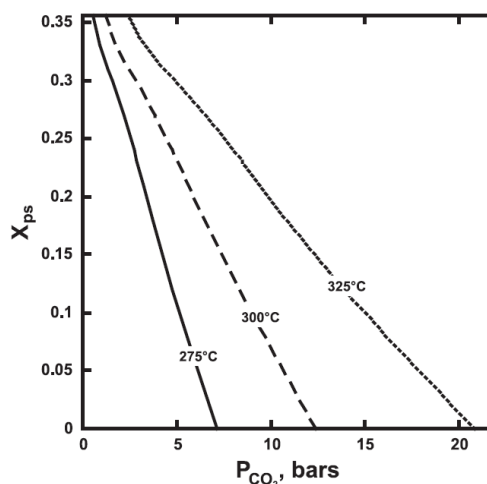

Figure 7: Compositional constraints between epidote composition (Xps) and the partial pressure of CO2,g at 275°, 300° and 325°C required by equilibrium for reaction (1) and equations (3) and (20)

7. EVALUATION OF LOCAL EQUILIBRIUM

Thermodynamic activities of aqueous species computed with the SOLVEQ and CHIM-XPT (Reed, 1982) computer programs for geothermal fluids are used to evaluate the extent to which the hydrothermal solutions are in equilibrium with the mineral assemblage epidote, prehnite, calcite and quartz (cf. reaction 1). The geothermal fluids are close to equilibrium with quartz, as illustrated in Figure 11a, where the symbols denote the activities of aqueous silica in the geothermal fluids and the solid line is the equilibrium constant for the quartz solubility reaction ($SiO_{2,quartz}$ == $SiO_{2,aq}$).

An alternate calculation of the saturation state of anhydrite provides some indication of the validity of our computed activities of Ca^{2+}. Anhydrite is a common hydrothermal mineral in the lower portions of the chlorite-epidote zone (Fig. 2; Lonker et al., 1993; Franzson et al., 2002; Marks et al., in review). The equilibrium constant for the anhydrite dissolution reaction:

$$CaSO_4 = Ca^{2+} + SO_4^{2-} \qquad (18)$$
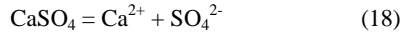
is shown in Figure 8b as a function of temperature at pressures equal to liquid-vapor equilibrium for H_2O. Symbols in the figure denote the ion activity product ($Q_{anhydrite}$) for reaction (18),

$$\log Q_{anhydrite} = \log (a_{Ca}^{2+} \bullet a_{SO4}^{2-}). \qquad (19)$$

Close correlation between the equilibrium constant (solid line) and values of the ion activity products (symbols) in Figure 8b suggest equilibrium between the geothermal fluids and anhydrite.
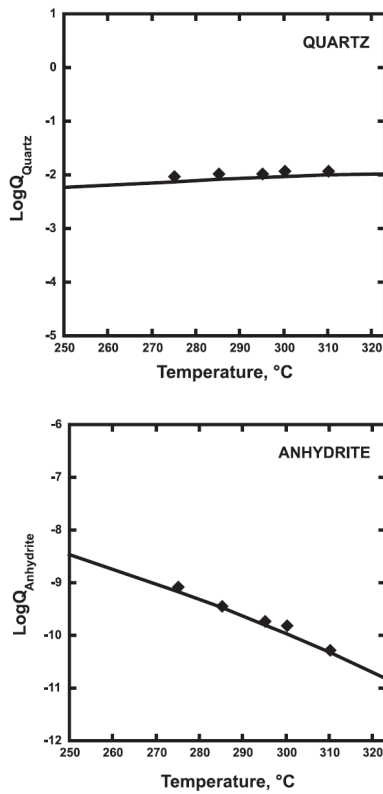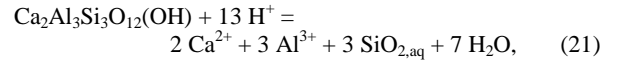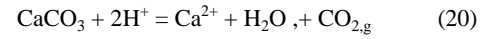

Figure 8: Saturation conditions for quartz (diagram a**) and anhydrite (diagram b) in the Reykjanes geothermal system based on distribution of aqueous species in measured geothermal fluids. Solid lines denote values of the equilibrium constant for the dissolution reactions and the symbols denote values of the molality of aqueous silica (represented as Log $m_{SiO2,aq}$ = Log Q_{quartz}, diagram** a**) and the value the ion activity product for reaction (18) as represented by equation (19) (diagram b)**

The saturation state of calcite, epidote and prehnite in the Reykjanes geothermal system is evaluated by employing the methodology represented in Figure 8 for quartz and anhydrite using the following hydrolysis reactions for calcite (CaCO3), epidote ($Ca_2Al_3Si_3O_{12}(OH)$) and prehnite ($Ca_2Al_2Si_3O_{10}(OH)_2$):

$$CaCO_3 + 2H^+ = Ca^{2+} + H_2O \text{,}+ CO_{2,g} \qquad (20)$$

$$Ca_2Al_3Si_3O_{12}(OH) + 13\,H^+ =$$
$$2\,Ca^{2+} + 3\,Al^{3+} + 3\,SiO_{2,aq} + 7\,H_2O, \qquad (21)$$

and

$$Ca_2Al_2Si_3O_{10}(OH)_2 + 10\,H^+ =$$
$$2\,Ca^{2+} + 2\,Al^{3+} + 3\,SiO_{2,aq} + 6\,H_2O \text{ . } \qquad (22)$$
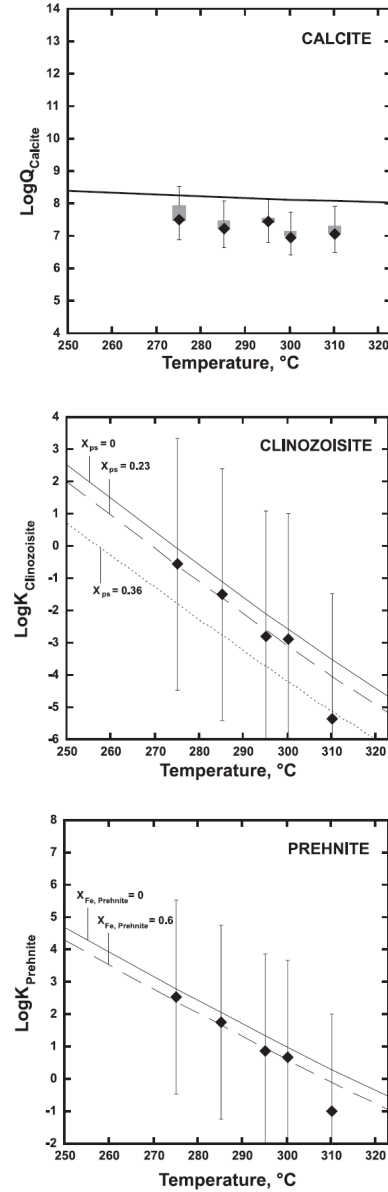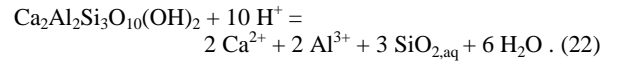

Figure 9: Saturation conditions for calcite (a)**, epidote** (b) **and prehnite** (c) **in the Reykjanes geothermal system based on the distribution of aqueous species for measured geothermal. Solid lines represent values of the equilibrium constant as a function of temperature for reactions (20), (21) and (22) and the symbols denote values of the ion activity products for these reactions (Eqn. 23). Error bars denote +/- 0.3 pH units. Broken lines in diagrams** b **and** c **denote isopleths for the noted compositions of epidote and prehnite solid solutions**

Values of the logarithm of the equilibrium constant for reaction (20), (21) and (22) are shown as solid lines in Figure 9 as a function of temperature (for pressures of

liquid-vapor equilibrium of H$_2$O). Symbols in the figure denote the ion activity products for measured geothermal fluids and defined by:

$$\log Q_j = \sum_i \log a_i^{\nu_i}, \qquad (23)$$

where Q$_j$ is the ion activity product of mineral component j (i.e. the Ca$_2$Al$_3$Si$_3$O$_{12}$ component in Fe(III)-Al epidote solid solutions for reaction 21, and the Ca$_2$Al$_2$Si$_3$O$_{10}$(OH)$_2$ component of Fe(III)-Al prehnite solid solutions for reaction 22), and a_i and ν_i are, respectively, the thermodynamic activity and stoichiometric reaction coefficient (positive for products and negative for reactants) of the ith aqueous species in reaction (20) thru (22). Values of log Q$_i$ for measured geothermal fluid compositions are represented by the diamond symbols in Figure 10. Error bars in the figure represent the assumed cumulative error of +/-0.3 in pH, but do not account for the <10% assumed error in values of measured P$_{CO2}$ compositions (cf. Figure 10a). Dashed lines in Figure 9b and 9c denote values of the equilibrium constant for reactions (21) and (22) that account for compositional variation of octahedral substitutions of Fe(III) and Al substitutions in the minerals epidote and prehnite, mathematically represented by the equilibrium constant relationship for chemical reactions (cf. Krauskopf and Bird, 1995).

The ion activity products for calcite (reaction 20) shown in Figure 9a indicate that calcite is in equilibrium with measured geothermal fluids (solid diamonds in the figure denote values of measured P$_{CO2}$ analyzed with SOLVEQ and the open rectangles represent the range in measured values analyzed using WATCH).

8. CORRELATION OF PREDICTED AND MEASURED FLUID P$_{CO2}$

Values of X$_{ps}$ used in calculating prehnite compositions are <0.36 as per the compositional constraints defined by the curve in Figure 9; only epidote samples that display an Fe(III) content equal to or less than the upper range of those which were observed to co-exist with prehnite (those displaying X$_{ps}$ values <0.36) were employed in this study for fluid P$_{CO2}$ calculations. In Figure 9, values of P$_{CO2}$ predicted from these measured epidote compositions (diamonds) can be compared with values of measured modern P$_{CO2}$ values as deduced from drillhole discharge fluids (open squares). Predicted fluid P$_{CO2}$ values using epidotes from cuttings where the aggregate assemblage of epidote, prehnite, calcite and quartz are observed range from 0.47 to 5.93 bars. Predicted values from cuttings where calcite and/or prehnite are absent from the assemblage range from 1.04 to 6.47 bars. The histograms of Figure 11 graphically represent the data presented in Figure 10 over the combined temperature range of 275° and 310°C; Figure 11a illustrates 117 epidote analyses from cuttings with the aggregate assemblage (Figure 6) over the temperature range of 275° to 310°C (purple bars; labeled calculated in the legend) compared with 74 computed P$_{CO2}$ values from geothermal fluids (blue bars labeled measured in the legend), and Figure 11b illustrates the same for 149 epidote compositions (Figure 4) where drill cuttings are missing at least one mineral of the epidote, prehnite, calcite and quartz assemblage (see Figures 2 and 4).
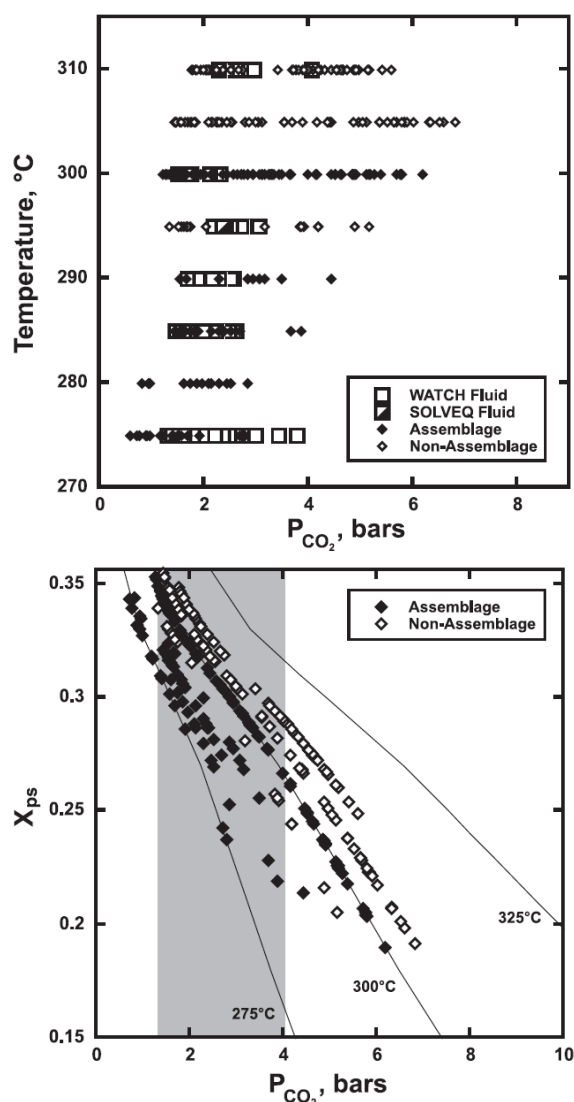

Figure 10: Compilation of: 1) calculated CO$_2$ partial pressures (diamonds) consistent with equilibrium for reaction (1), epidote and prehnite compositions reported in Figures 6 and 7 and equations, data and assumptions presented in the text, and 2) partial pressures of CO$_2$ determined from drillhole discharge fluids (see text for details) as a function of reference temperature in diagram a and measured epidote compositions from wells RN-9, RN-10 and RN-17 in diagram b. For definition of "Assemblage" and "Non-Assemblage" see Figure 5 caption. Solid lines in diagram b are from Figure 7, and the shaded rectangle corresponds to the range in measured P$_{CO2}$ values analyzed using WATCH

9. DISCUSSION

As a consequence of irreversible processes governing the dynamic nature of magma-hydrothermal systems one would *not* expect fluid-mineral equilibria to be attained in active geothermal systems. However, it was recognized during geothermal energy development in the 1960's that concentrations of aqueous silica, and alkali and alkaline Earth cations in geothermal fluids (from both drill hole discharge fluids and natural surface discharges, i.e. hot springs) systematically correlated with subsurface temperatures,
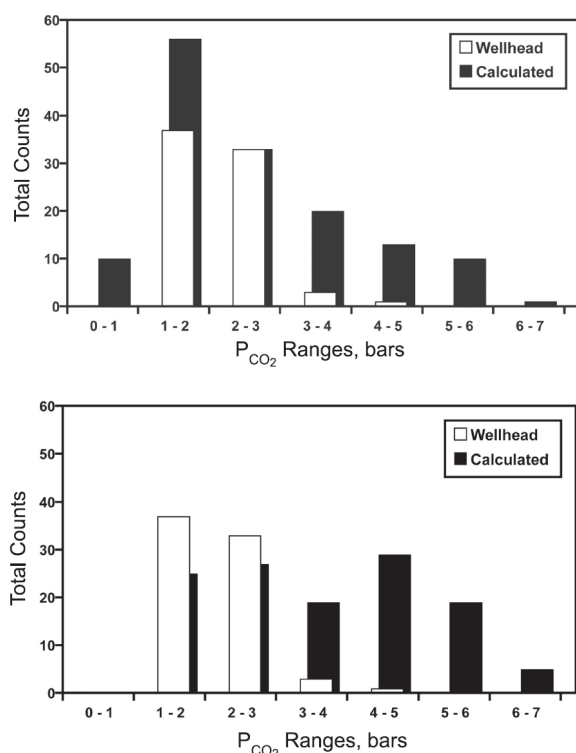
Figure 11: The partial pressures of CO_2 presented in Figure 10 represented as histograms of the number of analyses for: 1) calculated CO_2 partial pressures consistent with equilibrium for reaction (1), epidote and prehnite compositions reported in Figures 4 and 5 and equations (purple), and 2) measured partial pressures of CO_2 determined from drillhole discharge fluids (blue). Diagram a presents values of calculated partial pressures of CO_2 based on measured epidote compositions from drillhole cutting containing the assemblage epidote, prehnite and calcite (see Figs. 2 and 4), and diagram b for measured epidote compositions where either prehnite or calcite was not observed

thus providing a basis for solute geothermometers useful for geothermal exploration that are broadly consistent with solution-mineral equilibria (cf. Fournier and Rowe, 1962; Arnórsson, 1970, 1985; Fournier, 1977; Fournier and Truesdell, 1973; Fournier and Potter, 1979, 1982; Arnórsson et al., 1983). These relationships provide empirical evidence that many high-temperature geothermal fluids (>~250°C) approach equilibrium with secondary quartz, feldspars and calc-silicates, despite theoretical inferences of irreversible transport phenomena and reaction, as well as petrographic evidence of paragenetic complexity including compositional zoning and replacement textures among hydrothermal minerals.

As with aqueous silica, and alkali and alkaline Earth cations in geothermal fluids, similar systematic relationships have been reported between empirical and theoretical values for the concentration of CO_2. For example, a close correlation has been noted between CO_2 concentrations in geothermal fluids and values computed for equilibrium among alkali feldspars, epidote, layer-silicates (illite/muscovite) and calcite for geothermal systems in silicic volcanic rocks (Taupo Volcanic Zone, New Zealand; Giggenbach, 1981) and in calcareous sediments (Salton Sea geothermal system, California; Bird and Norton, 1981). In basaltic rocks Stefánsson and Arnórsson (2002) found that CO_2 concentrations estimated using reaction (1) are within an

order of magnitude of measured CO_2 partial pressures in many Icelandic geothermal systems. Similar results have been obtained for aquifer fluids in geothermal fields at Momotombo in Nicaragua (Arnórsson, 1996), Zunil in Guatemala (Arnórsson, 1995), and Svartsengi in Iceland (Giroud unpublished work).

In the present study, we have built upon this previous body of research to evaluate the extent to with local equilibrium of the mineral assemblage of epidote, prehnite, quartz, and calcite with geothermal fluids buffers the concentration of CO_2. Our study illustrates that thermodynamic calculations of CO_2 concentrations required for local equilibrium of this assemblage is a sensitive function of compositional variations in epidote and prehnite (Fig. 7). Any quantitative comparative analysis of P_{CO2} computed from drill hole discharge fluids with values computed from equilibrium constraints imposed by reaction (1) must be viewed in terms of the nature of the samples analyzed. For the geothermal fluids, we note that discharge fluids are typically produced from a number of different input feed points within the drill hole, and thus sample different portions of the geothermal reservoir, and that the uncertainty of P_{CO2} of the geothermal reservoir fluid computed from chemical analyses of steam and liquid discharge is in itself dependent upon a combination of factors related to sampling, analytical and thermodynamic procedures. Likewise, mineralogic phase relations are based on petrographic studies of drillhole cuttings that are typically <2mm in size, and essentially represent a scattered sample of the crushed lithology produced during drilling, which precludes detailed analysis of paragenetic relationships among minerals and mineralized vein systems.

With these limitations in mind, we note that the measured fluids are saturated with respect to quartz (Fig. 8a), epidote (Fig. 9b) and prehnite (Fig. 9c). In terms of our adopted uncertainty of pH of +/-0.3, calcite is saturated, or at most slightly undersaturated with respect to the geothermal fluids over the temperature range of 275° to 310°C (Fig. 9a), which represents the range of reference temperatures for our fluid analyses. Within these temperatures, values of P_{CO2} determined by chemical analysis of discharge fluids vary between ~1.3 to 4 bars (Fig. 10a); this range decreases with increasing temperature (Fig. 10a), but this may well be a sampling bias due to the larger number of lower-temperature samples analyzed. As a consequence, the shaded area in Figure 11b corresponds to the overall range of measured P_{CO2} values of ~1.3 to 4 bars. The diamonds in Figure 14b denote values of P_{CO2} computed from individual epidote analyses using equations and data presented above over the reference temperature of 275° to 310°C. The solid diamonds (Assemblage) represent analyses of epidote crystals from drill cutting that contain the assemblage epidote + prehnite + calcite + quartz (see Figs. 2 and 4), whereas the open diamonds (Non-Assemblage) are analyses from drill cuttings where prehnite and/or calcite are not observed. Of the 117 epidote analyses from cuttings containing the assemblage epidote + prehnite + calcite + quartz (Fig. 11b) 74% of the computed values of P_{CO2} are within the measured range of P_{CO2} (1.3 to 4.0 bars), this is graphically illustrated in the histogram of Figure 12a. These computed "assemblage" values range from ~0.5 to 6 bars. In contrast, of the 149 epidote analyses from drill cuttings that do not contain prehnite and/or calcite, 62% of the computed values of P_{CO2} are within the measured range (see Fig. 11b). These computed "non-assemblage" values range from ~1 to ~6.5 bars. If calcite is absent from the assemblage, the computation of P_{CO2} using equilibria for reaction 1 provides the maximum value of P_{CO2} at which calcite will not be

present. Thus, our method for calculating fluid P_{CO2} is proven quite reliable when all four index minerals of the epidote-prehnite-calcite-quartz assemblage are present. Additionally, if only epidote, prehnite and quartz are observed, our method still serves as a moderately accurate predictive proxy for fluid P_{CO2} values in the Reykjanes geothermal system.

There are several possible explanations for values of P_{CO2} that are greater than the measured values of the present day geothermal fluids (shaded area in Fig. 10b). If calcite is not present in the assemblage (that is, the fluid is undersaturated with respect to calcite) then the computed value of P_{CO2} (diamonds in Fig. 10b) denotes a maximum value required for the absence of calcite. As the samples analyzed are drill cuttings, the presence of calcite in the cuttings does not necessarily require paragenetic equivalence with other mineral phases in the cuttings sample. We can see from Figure 10b that epidotes denoted by the solid diamonds (Assemblage) that have values of P_{CO2} > 4 bars are Al-rich epidotes (Xps <0.25) and at temperatures close to 300°Ç. If calcite is not in equilibrium with epidote, prehnite and quartz in these samples then the high P_{CO2} would represent a theoretical maximum values. However, if equilibrium for the assemblage is established then alternate explanations are required, such as local increases in P_{CO2} due to magmatic intrusions (dikes). This alone highlights the importance of obtaining drill cores for evaluation of paragenetic relations of hydrothermal minerals in active geothermal systems.

Although complex chemical zoning is observed in epidotes from the Reykjanes geothermal system, there is a general trend for the formation of Fe(III)-rich cores and Al-rich rims. If this zoning is formed while equilibrium is maintained among epidote + prehnite + calcite + quartz + fluid then the thermodynamic relationships illustrated in Figures 7 and 10b provide possible explanations. For example, if the zoning for Fe(III)-rich core to Al-rich rim occurs under near isothermal conditions this would require an increase in P_{CO2} with time. The rise in CO_2 content may likely record an increase in the number of high-level intrusions of dikes/sills and their magmatic degassing during the geologic evolution of this geothermal system. The most recent eruption on the Reykjanes peninsula was in AD 1226 and most of the peninsula is covered by Holocene lavas and also by subglacial hyaloclastites (Saemundsson, 1997). Alternatively, if the zoning occurs under conditions of near constant P_{CO2}, then equilibrium constraints imposed by reaction (1) requires that temperature decreases (see Fig. 10b). The latter is likely in portions of the geothermal system as suggested by suppressed geotherms in well RN-17 relative to the high-temperature mineral zoning shown in Figure 2.

CONCLUSION

This study developed a method for calculating fluid P_{CO2} in the Reykjanes geothermal system based on epidote compositions. This method has proven quite reliable when all four index minerals (epidote, prehnite, quartz, calcite) are present at the same depth, predicting fluid compositions in excellent agreement with measured modern fluids. Additionally, if only epidote, prehnite and quartz are observed, our data demonstrates that predicted fluid P_{CO2} compositions are still in moderately good agreement with measured fluids in the Reykjanes system. Ultimately, the correlation between measured and predicted fluid compositions, provides insight into future abilities to characterize spatial and temporal concentrations of CO_2 in active and fossil hydrothermal and low-grade metamorphic environments in mafic lithologies based on compositional variations and paragenesis of hydrothermal minerals. In addition, this study will aid in understanding the nature of reactions that involve natural sequestration of CO_2 derived from magmatic degassing, and injection of industrial CO_2-rich fluids within hydrothermal environments in basaltic rocks.

REFERENCES

Arnason J. G., Bird D. K., and Liou J. G.: Variables controlling epidote composition in hydrothermal and low-pressure regional metamorphic rocks, *Abhandlungen der geologischen Bundesantalt*, **49**, (1993), 17–25.

Arnórsson S.: Underground temperatures in hydrothermal areas in Iceland as deduced from the silica content of the thermal water , *Geothermics*, **2**, (1970), 536-41.

Arnórsson S.: Major element chemistry of the geothermal sea-water at Reykjanes and Svartsengi, Iceland, *Mineralogical Magazine*, **42**, (1978), 209-220.

Arnórsson, S.: The use of mixing models and chemical geothermometers for estimating underground temperatures in geothermal systems, *J. Volcanol. Geotherm. Res*., **23,** (1985), 209-335.

Arnórsson S.: Geothermal systems in Iceland; structure and conceptual models; I, High-temperature areas:, *Geothermics*, **24**, (1995), 561–602.

Arnórsson S.: Interpretation of chemical and isotopic data on fluids discharges from wells in the Momotombo geothermal field, Nicaragua, *International Atomic Energy Agency*, (1996), 21 p.

Arnórsson S. and Gunnlaugsson E.: New gas geothermometers for geothermal exploration-calibration and application, *Geochimica et Cosochimica Acta*, **49**, (1985), 1307-1325.

Arnórsson S., Stefansson A, and Bjarnason J.O.: Fluid-Fluid Interactions in Geothermal Systems, *Reviews in Mineralogy & Geochemistry*, **65**, (2007), 259-312.

Arnórsson, S., Gunnlaugsson, E., and Svavarsson, H.: The chemistry of geothermal waters in Iceland-III. Chemical geothermometry in geothermal investigations, *Geochim. Cosmochim. Acta*, **47,** (1983), 567-577.

Bird D. K. and Norton D. L.: Theoretical prediction of phase relations among aqueous solutions and minerals: Salton Sea geothermal system, *Geochim Cosmochim Acta*, **45,** (1981), 1479-1493.

Bird, D. K., and Helgeson H. C.: Chemical interaction of aqueous solutions with epidote-feldspar mineral assemblages in geologic systems: I. Thermodynamic analysis of phase relations in the system CaO-FeO-Fe_2O_3-Al_2O_3-SiO_2-H_2O-CO_2, *American Journal of Science*, **280**, (1980), 907-941.

Bird D. K., Schiffman P., Elders W. A., Williams A. E., and McDowell S. D.: Calc-silicate mineralization in active

geothermal systems: Economic Geology, **79**, (1984), 671-695.

Bird D. K., Cho M., Janik C. J., Liou J. G., and Caruso L. J.: Compositional, order/disorder, and stable isotope characteristics of Al-Fe epidote, State 2-14 drill hole, Salton Sea geothermal system, *Journal of Geophysical Research*, **93**, (1988), 13135-13144.

Bird D. K., and Spieler A. R.: Epidote in geothermal systems, *Reviews in Mineralogy and Geochemistry*, **56**, (2004), 235-300.

Bjarnason J. O.: The speciation program WATCH version 2.1A, *Icelandic National Energy Authority Report*, (1994).

Conrad C. P., Lithgow-Bertelloni C., and Louden K. E.: Iceland, the Farallon Slab, and the Dynamic Topography of the North Atlantic, *Geology*, **32**, (2004), 177-180.

Deer W. A., Howie R. A., and Zussman J.: Rock-forming minerals, v.1, Ortho and Ring Silicates: New York, John Wiley & Sons, Inc., (1962), 333 p.

Dollase W. A.: Mossbauer spectra and iron distribution in the epidote group minerals, *Zeitschrift fuer Kristallographie*, **138**, (1973), 41-63.

Fournier, R. O.: Chemical Geothermometers and Mixing Models for Geothermal Systems, *Geothermics*, **5,** (1977), 41-50.

Fournier, R. O. and Potter, R. W., II: Magnesium correction to the Na-K-Ca chemical geothermometer, *Geochim. Cosmochim. Acta*, **43,** (1979), 1543-1550.

Fournier, R. O. and Potter, R. W., II: A revised and expanded silica (quartz) geothermometer. *Geotherm. Resourc. Counc. Bull.*, **11**, (1982), 3-12.

Fournier, R. O. and Rowe, J. J.: The solubility of amorphous silica in water at high temperatures and pressures, *American Mineralogist*, **62**, (1962), 1052-1056.

Fournier, R. O. and Truesdell, A. H.: An empirical Na-K-Ca geothermometer for natural waters, *Geochim. Cosmochim. Acta*, **37,** (1973), 1255-1275.

Franzson H.: Reykjanes. Rannsóknir á vökvabólum í útfellingum í holum RN-9 og RN-10, *Orkustofnun Report*, **021**, (2000), 1-20. (in Icelandic).

Franzson H., Thordarson S., Björnsson G., Gudlaugsson S. T., Richter B., Fridleifsson G. O., and Thorhallsson S.: Reykjanes high-temperature field, SW-Iceland. Geology and hydrothermal alteration of well RN-10, *Proceedings,* 27th Workshop on Geothermal Reservoir Engineering. Stanford University, Stanford, California (2002).

Fridleifsson G. O., Blischke A., Kristjánsson B. R., Richter B., Einarsson G. M., Jónasson H., Franzson H., Sigurdsson O., Danielsen P. E., Jónsson S. S., Thordarson S., Thórhallsson S., Hardardóttir V., and Egilson Th.: Reykjanes Well Report RN-17 & RN-17ST, *ISOR*, **007**, (2005).

Giggenbach W. F. Geothermal mineral equilibria, *Geochimica et Cosmochimica Acta*, **45**, (1981), 393-410

Giuli G., Bonazzi P., and Menchetti S.: Al-Fe disorder in synthetic epidotes: a single-crystal x-ray diffraction study, *Am. Mineral.*, **84**, (1999), 933-936.

Gottschalk, M.: Thermodynamic properties of zoisite, clinozoisite, and epidote, *Reviews in mineralogy and geochemistry*, eds. a. leibschert and b.franz,, **50**, (2004), 83-124.

Hashimoto M.: The chemistry and optics of prehnite, *The Journal of the Geological Society of Japan*, **70**, (1964), 180-183.

Helgeson H. C., Nesbitt H. W., and Bird D.K.: Summary and critique of the thermodynamic properties of rock-forming minerals, *Am J Sci*, **278a**, (1978), 1-229.

Hjartarson A.: Reiknilíkan af jardhitakerfinu á Reykjanesi og spár um vidbrögd þess vid 100 MW rafmagns-framleidslu: ISOR report in preparation, (2006). (Reservoir modelling on the Reykjanes geothermal system and predicted response to 100 MWe production).

Hjartarson A., and Juliusson E.: Reiknilíkan af jarðhitakerfinu á Reykjanesi og spár um viðbrögð þess við 100 MW rafmagns-5 framleiðslu. Íslenskar orkurannsóknir, *ÍSOR*, **2007/025,** (2007). 145 p. (in Icelandic)

Holland T. J. B. and Powell R.: An internally-consistent thermodynamic dataset for phases of petrological interest, *Journal of Metamorphic Geology*, **16**, 309-344.

Johnson J. W., Oelkers E. H., and Helgeson H. C.: Supcrt92: A software package for calculating the standard molal thermodynamic properties of minerals, gases, aqueous species, and reactions from 1 bar to 5000 bar and 0 degrees Celsius to 1000 degrees Celsius, *Computational Geosciences*, **18**, (1992), 899-947.

Klein C.: The 22nd edition of the Manual of Mineral Science (after J.D. Dana): New York, John Wiley & Sons, Inc., (2002), 641 p.

Krauskopf K. B., and Bird D. K.: Introduction to Geochemistry: San Francisco, McGraw Hill, (1995), 668 p.

Larsen G., Gudmundsson M. T., and Bjornsson H.: Eight centuries of periodic volcanism at the center of the Iceland hotspot revealed by glacier tephrostratigraphy, *Geology*. **26**, (1998), 943-946.

Lonker S. W., Franzson H., and Kristmannsdóttir H.: Mineral-fluid interactions in the Reykjanes and Svartsengi geothermal systems, Iceland, *American Journal of Science*, **293**, (1993), 605–670.

Marks N., Schiffman P., Zierenberg R., Elders W., and Fridleifsson G.: Iceland Deep Drilling Project: (VI) Fluid-rock interactions in the Reykjanes Geothermal System as indicated by alteration mineralogy and sulfur isotopes, *American Geophysical Union, Fall Meeting 2006*, **Abstract #NG43A-1150**, (2006).

Marty B., and Tolstikhin I. N.: CO_2 fluxes from mid-ocean ridges, arcs and plumes, *Chemical Geology*. **145**, (1998), 233-248.

Milodowski A. E., Savage D., Bath A. H., Fortey N. J., Nancarrow P. H. A., Shepherd T. J.: Hydrothermal mineralogy in geothermal assessment: Studies of Miravalles Field, Costa Rica and experimental simulations of hydrothermal alteration, *British Geological Survey Technical Report WE/89/63*, **Fluid Processes Group Series: 81-82**, (1989).

Freedman et al.

Mungania J.: Borehole geology of well RN-9, Reykjanes, SW-Iceland, *United Nations Training Programme, Reykjavik, Iceland*, **12**, (1993), 1-38.

Pálmason G., Johnsen G. V., Torfason H., Saemundsson, K., Ragnars K., Haraldsson G. I., and Halldórsson G. K.: Evaluation of geothermal resources in Iceland, *National Energy Authority Report OS-85076/JHD-10*, (1985), 134 p. (in Icelandic).

Patrier P., Beaufort D., Meunier A., Eymery J. P., and Petit S.: Determination of nonequilibrium ordering state in epidote from the ancient geothermal field of Saint Martin: Application of Mössbauer Spectroscopy, *Am Min*, **76**, (1991), 602-610.

Ragnarsdóttir K. V., Walther J. V., and Arnórsson S., 1984, Description and interpretation of the composition of fluid and alteration mineralogy in the geothermal system, at Svartsengi, Iceland, *Geochimica et Cosmochimica Acta*, **48**, (1991), 1535-1553.

Reed M.H.: Calculation of multicomponent chemical equilibria and reaction progress in systems involving minerals, gases and an aqueous phase, *Geochimica et Cosmochimica Acta*, **46**, (1982), 513-528.

Robie R. A., and Hemingway B. S.: Thermodynamic properties of minerals and related substances at 298.15 K and 1 bar (10^5 Pascals) pressure and at higher temperatures, *U. S. Geol. Surv. Bull.*, **2131**, (1995), 461 p.

Saemundsson K.: Simplified geological and geothermal map of Reykjanes: Prepared by Okustofnun for Sudurnes Regional Heating, scale 1:10,000, (1997).

Sleep N. H., and Zahnle K.: Carbon dioxide cycling and implications for climate on ancient Earth, *Journal of Geophysical Research*, **106**, (2001), 1373-1399.

Stefánsson A., and Arnórsson S.: Gas pressures and redox reactions in geothermal fluids in Iceland, *Chemical Geology*, **190**, (2002), 251–271.

Surdam R. C.: Electron microprobe study of prehnite and pumpellyite from the Karutsen group, Vancouver Island, British Columbia, *American Mineralogist*, **54**, (1969), 256-266.

Sveinbjörnsdóttir Á. E.: Composition of geothermal minerals from saline and dilute fluids-Krafla and Reykjanes, Iceland, *Lithos*, **27**, (1992), 301–315.

Tómasson J., and Kristmannsdóttir H.: High temperature alteration minerals and thermal brines, Reykjanes, Iceland, *Contributions to Mineralogy and Petrology*, **36**, (1972), 123-134.

White R., and Morton A.: The Iceland Plume and its influence on the evolution of the NE Atlantic: *Journal of the Geological Society*, **152**, (1995), 935-941.